Electronic Supplementary Information for

Fabrication of a monolithic cryogel from cyclohexane organogel of coordination polymer based on a phosphoester

Yuiko Tasaki-Handa*‡, Yukie Abe, and Kenta Ooi

Environmental Management Research Institute, National Institute of Advanced Industrial Science and Technology (AIST)
Onogawa 16-1, Tsukuba, Ibaraki, Japan

‡Present address: Graduate School of Science and Technology, Saitama University, 255 Shimo-Okubo, Sakura-ku, Saitama-shi, Japan

1. Synthesis and preparation of [Ln(dehp)₃], organogels, and cryogels

1-1. [Ln(dehp)₃] (Ln=Ce, Sm, Dy, or Yb)

Di-(2-ethylhexyl) phosphoric acid (HDEHP, Figure S1(A)) was converted to sodium di-(2-ethylhexyl) phosphate (NaDEHP): HDEHP in methanol and equimolar amounts of aqueous NaOH were mixed to obtain 0.3 M NaDEHP in 90:10 vol% methanol–water (α). [Ln(dehp)₃] was synthesized by mixing α and aqueous 0.2 M LnCl₃ aq (β) at an α:β ratio of 2:1. The whitish precipitate was filtered after one day, washed with 90:10 vol% methanol–water several times, and dried at room temperature. The highest available grade for HDEHP (97%, Sigma-Aldrich) and SmCl₃ 6H₂O (Wako Pure Chemical Industries) was obtained and used as received.

The C and H content in ca. 5 mg [Ln(dehp)₃] was measured using an organic elemental analyzer (Thermo SCIENTIFIC, FLASH 2000). For the Ln and P content, the [Ln(dehp)₃] (ca. 15 mg) was decomposed in HNO₃ (60%, 3 mL)–and–H₂O₂ (30%, 0.3 mL) under microwave irradiation, following which the concentration of Ln and P was measured using inductively coupled plasma-optical emission spectroscopy (ICP-OES, Shimadzu ICPE-9000). Table S1 summarizes the element content.

1-2. Organogels

Approximately 0.1 g of the [Ln(dehp)₃] (Ln=Ce, Sm, Dy, or Yb) was placed in a glass vial (6 mL) with 3 mL of cyclohexane and left to settle for three days at 20 °C ((a) 0.50, (b) 0.75, (c) 1.5, (d) 3.0, or (e) 6.0 mL of cyclohexane only for [Sm(dehp)₃]). The [Ln(dehp)₃] instantly absorbed the cyclohexane and became a transparent gel; however, three days were required for the gel to appear homogeneous.

The [Sm(dehp)₃] gel in the glass vial was rapidly frozen in liquid nitrogen and placed in a cooled flask. The flask was capped with a silicon plug connecting to a rotary pump through a cold trap and placed under -100 °C in a Dewar vessel for 2 h (Figure S2). After which, the gel was dried for 72 h. The temperature could not be controlled but was monitored. Figure S3 shows the change in the temperature in a Dewar vessel.
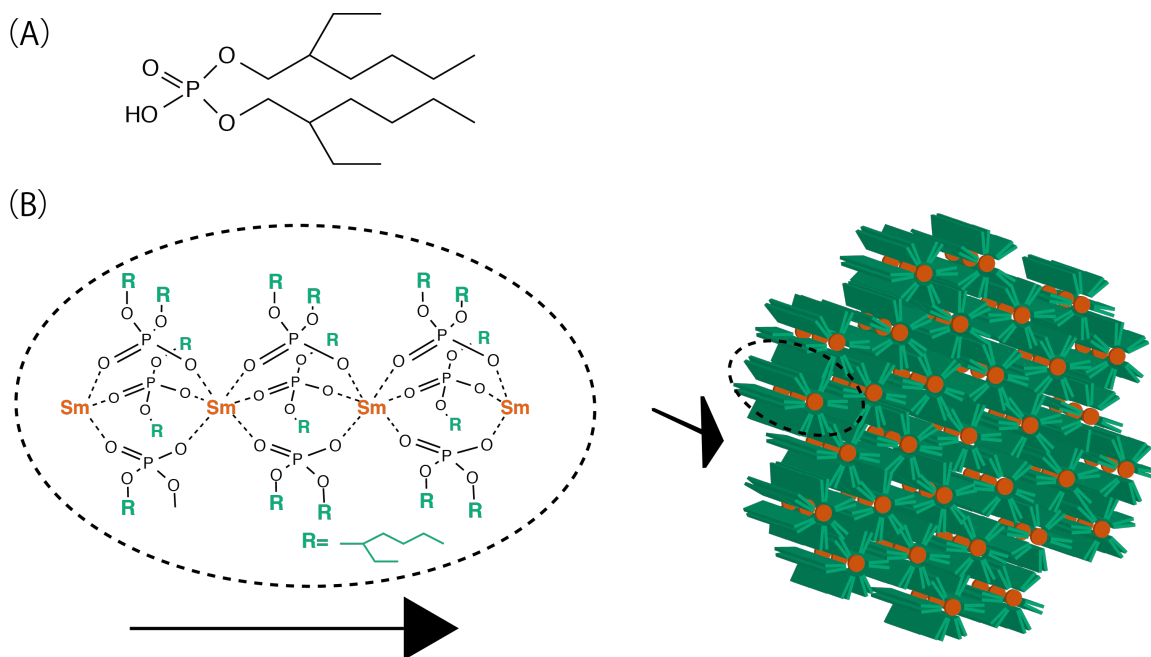
(A)

(B)

Figure S1　Schematic of a HDEHP molecule (A) and [Sm(dehp)₃] (B). The arrows in (B) indicate linear chains with three O–P–O bridges between Sm^{3+}. The O–P–O bridging moiety is not included in the figure on the right side in (B).

Table S1　Element contents (wt%) in the precipitates

	C	H	Ln	P
Ce	51.64 (52.50)	9.55 (9.31)	14.00 (12.69)	8.36 (8.41)
Sm	49.52 (51.72)	9.38 (9.22)	15.06 (13.49)	8.19 (8.33)
Dy	49.12 (51.17)	9.17 (9.12)	16.06 (14.42)	8.01 (8.24)

* Calculated values for [Ln(dehp)₃] are shown in parenthesis.
** C and H contents were determined by elemental analysis;　Ln and P were determined by ICP-OES after acid digestion.
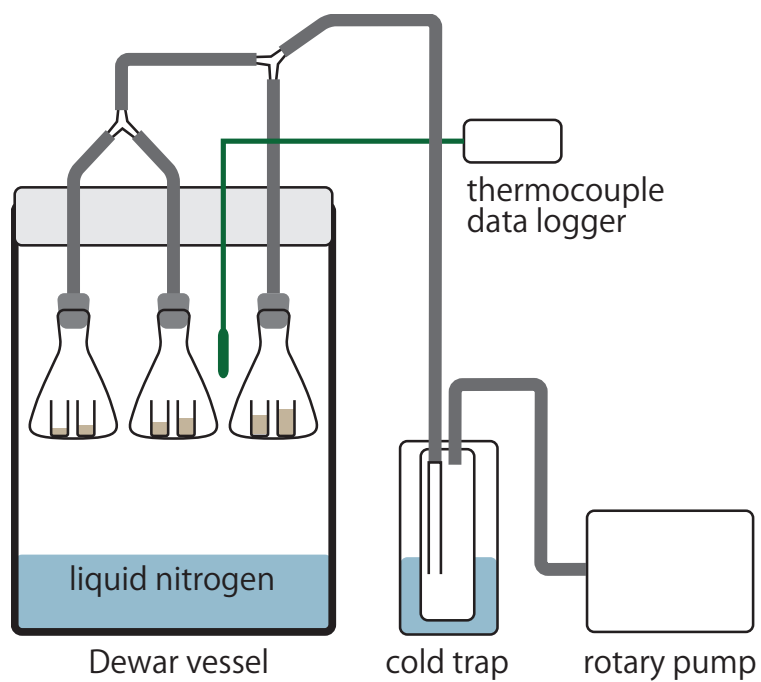
Figure S2　　　　Schematic of the set up for lyophilization of cyclohexane organogels.
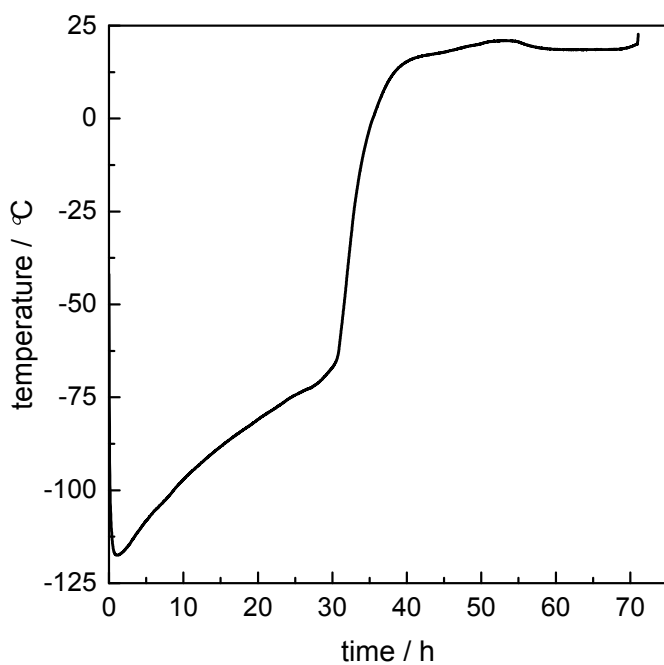

Figure S3　Temperature change during lyophilization.

2. Dependence of R on organic solvent

The gelation of [Ce(dehp)₃] was tested in various organic solvent shown in Table S2. The R represents the volume ratio of the organic solvent to cyclohexane. Although it has not been elucidated what is the important factor to form organogel, there is a trend that solvents of the larger ε_r, δ, and log P_{ow} are well absorbed in [Ce(dehp)₃], however, n-octane and n-dodecane are exceptional.

Table S2   Dependence of R on some parameters of organic solvent

	dielectric constant (ε_r)	hildebrand parameter (δ)*	log P_{ow}	R
n-pentane	1.837	14.3	3.39	74.3
n-hexane	1.887	14.9	3.90	69.5
n-heptane	1.921	-	4.66	59.3
n-octane	1.948	15.6	5.18	×
n-dodecane	2.012	16.2	6.8	×
cyclohexane	2.024	16.8	3.4	54.8
1,4-dioxane	2.219	-	-0.27	×
toluene	2.379	18.2	2.7	×

* C. Reichardt and T. Welton, "Solvents and Solvent Effects in Organic Chemistry", fourth edition, WILEY-VCH.
** "×" represents that cyclohexane was not absorbed.

3. Characterization of [Ln(dehp)₃], organogels, and cryogels

The morphologies of the as-synthesized and lyophilized [Sm(dehp)₃] were observed using a scanning electron microscopy (SEM, JOEL JSM-6010LA). The applied energy was adjusted to a range of 10–15 keV. The samples were coated with platinum before imaging (Hitachi, E-1030 Ion Sputter).

Powder X-ray diffraction (PXRD) was used to determine the structure of the as-synthesized material, the organogels, and the cryogels with a powder X-ray diffractometer (Bruker, D2PHASER). The gels containing cyclohexane were covered with Mylar film during the measurements. As shown in Figure S4, the gel **a** shows a weak peak in its pattern, while there are no peaks for the gels **b–e** due to their low density. The d values for the peaks at 2θ ~ 5.4° for the as-synthesized [Sm(dehp)₃] and gel **a** are 16.7 Å, which are likely to correspond to the nearest Sm^{3+}–Sm^{3+} distance.

This indicates that the packing of the O–P–O bridged linear chains in [Sm(dehp)₃] became less close after absorbing cyclohexane in the gelatinous state. Since the difference was only 0.5 Å, this slight structural change should not be directly associated with cyclohexane absorption. In other

words, cyclohexane molecules should still predominantly be present outside of the crystalline domains.   The patterns in a 2θ range of 3–40° for the as-synthesized [Sm(dehp)$_3$] and cryogels are shown in Figure 2 in the main article.

Figure S5   compares the PXRD patterns of [Ln(dehp)$_3$] (Ln=Ce, Sm, Dy, or Yb). For each pattern, there is a broad peak at 2θ~23°. The broad peak and the other peaks were devided, and the ratio of their peak area was determines using TOPAS software (Bruker AXS). The results are summarized in Figure 5 in the main manuscript.
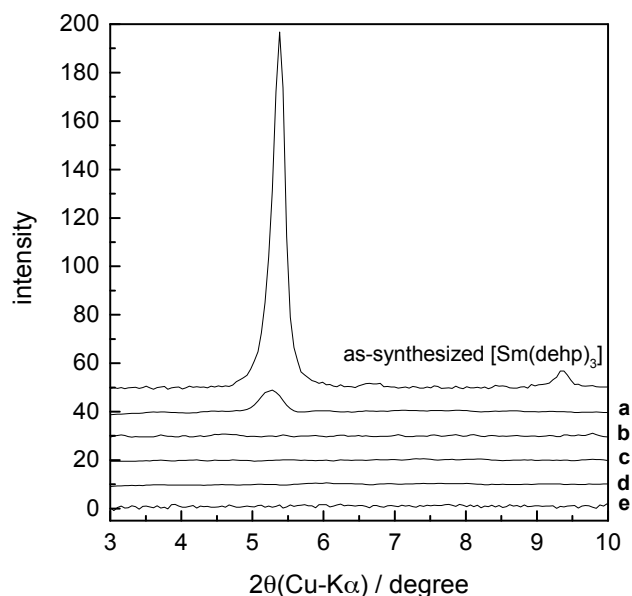

Figure S4   PXRD patterns of the as-synthesized [Sm(dehp)$_3$] and of organogels (**a–e**) in the 2θ range of 3–10°.
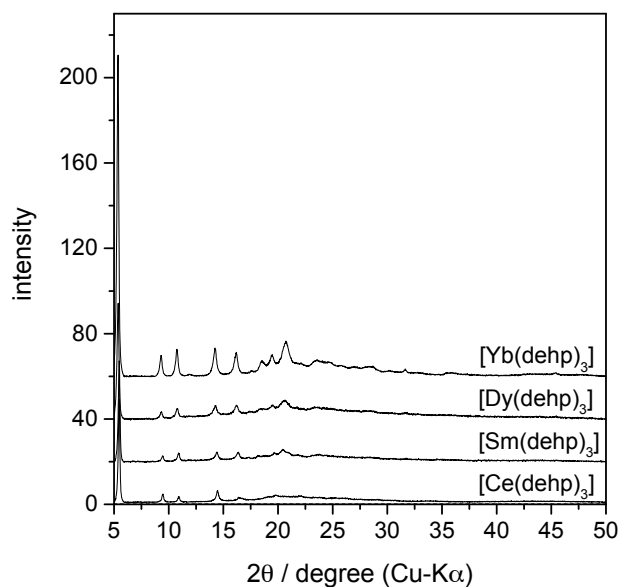

Figure S5 PXRD patterns of [Ln(dehp)$_3$] (Ln=Ce, Sm, Dy, or Yb) in the 2θ range of 5–50°.

4. *X-ray absorption fine structural (XAFS) analysis*

XAFS analysis was conducted for the as-synthesized and the gels **b** and **c**. XAFS spectra at the K-edge of Sm (46.846 keV) were collected in transmission mode at beamline BL11XU of SPring-8 (Harima, Japan). The operating energy and the ring current were 8 GeV and 99 mA, respectively. Si(311) was used as a monochromator. The optics and XAFS measurement systems in the beam line are described in the literature.[2] The intensities of the incident (I_0) and transmitted (I) X-rays were detected by using ionization chambers filled with Ar (50%) + N_2 (50%). The XAFS oscillation $\chi(k)$ was extracted from the XAFS spectra using the Athena software package for XAS analysis: subtraction of a linear pre-edge background, normalization, and conversion to k-space, followed by μ_0 fitting using a cubic spline.

Figures S6(A), (B), and (C) show the normalized $\mu(E)$, $\chi(k)k^3$, and |FT| spectra, respectively for the as-synthesized [Sm(dehp)$_3$] and the organogels **b** and **c**. The spectra are all consistent with each other, indicating that the local structure of Sm^{3+} remains in a gelatinous state.
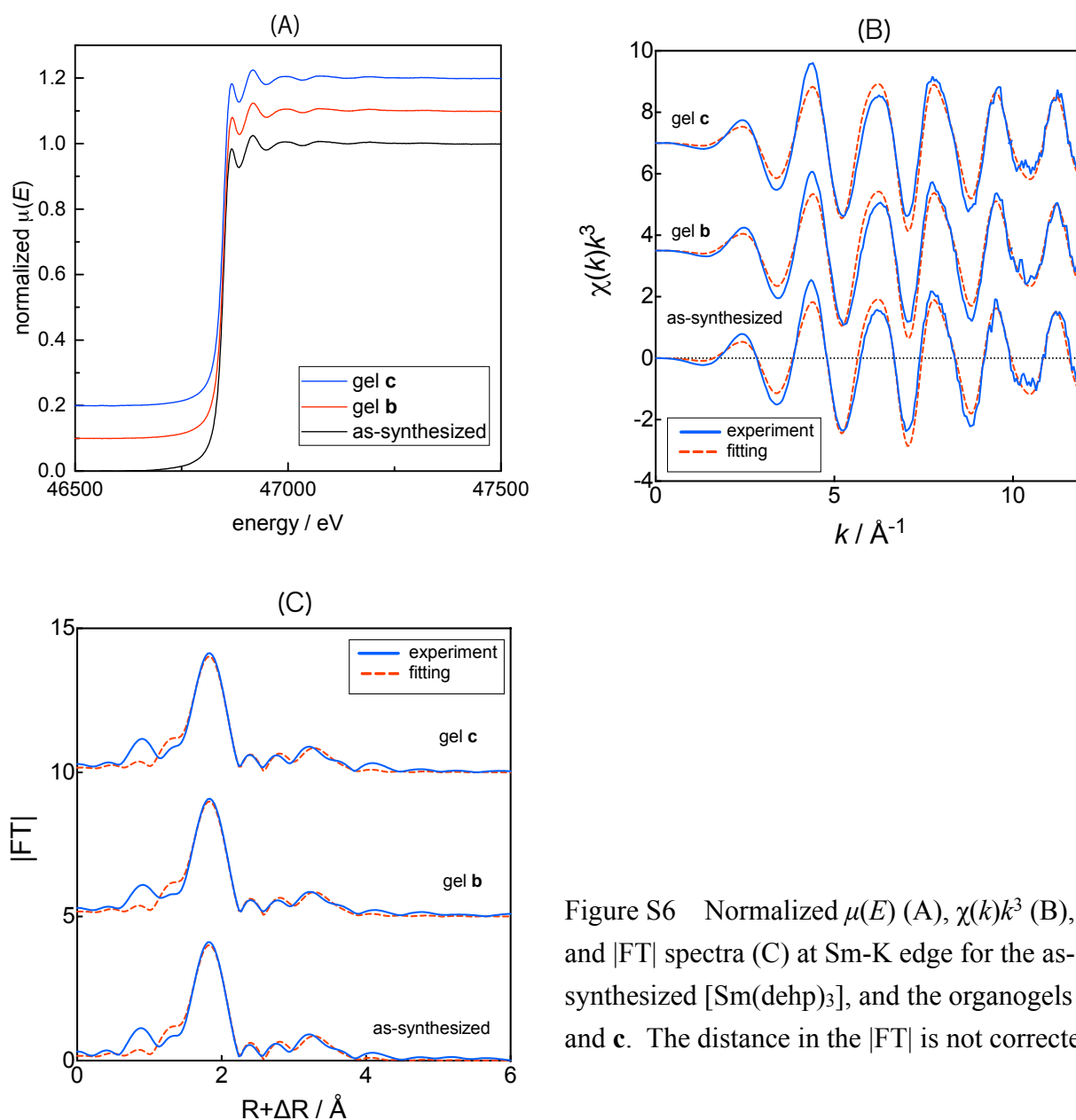

Figure S6　Normalized $\mu(E)$ (A), $\chi(k)k^3$ (B), and |FT| spectra (C) at Sm-K edge for the as-synthesized [Sm(dehp)$_3$], and the organogels **b** and **c**. The distance in the |FT| is not corrected.

Table S3　　XAFS curve-fits parameters

	ΔE /eV	Ln-O distance / Å	Ln-P distance / Å	ss (O)	ss (P)	R factor
as-synthesized	-2.52 ± 0.90	2.32 ± 0.0042	3.86 ± 0.011	0.0049 ± 0.00022	0.0095 ± 0.0010	0.0163
gel **b**	-2.00 ± 0.75	2.32 ± 0.0035	3.86 ± 0.0095	0.0050 ± 0.00018	0.0095 ± 0.00091	0.0181
gel **c**	-2.44 ± 1.46	2.32 ± 0.0067	3.68 ± 0.019	0.0049 ± 0.00035	0.0095 ± 0.0018	0.0160

The FT data shows two peaks: an intense one around 1.8 Å (not phase-corrected) attributed to the nearest O neighbors, and another around 3.2 Å (not phase-corrected) attributed to P atom. Table S3 summarizes the curve-fits parameters: the coordination number was set as six. The Ln–O distances agree with the sum of ionic radii (r) of oxygen and six-coordinated Ln^{3+}.

5. *N_2 absorption isotherm*

　　The adsorption of N_2 at the temperature of liquid nitrogen was measured with a high precision gas/vapor adsorption measurement instrument (MicrotracBEL, BELSORP max) for the as-synthesized [Sm(dehp)$_3$] and cryogels **A–E**. For the as-synthesized [Sm(dehp)$_3$], the volume of the adsorbed N_2 (V_a) apparently increases with p/p_0 when p/p_0 is higher than 0.9. According to the
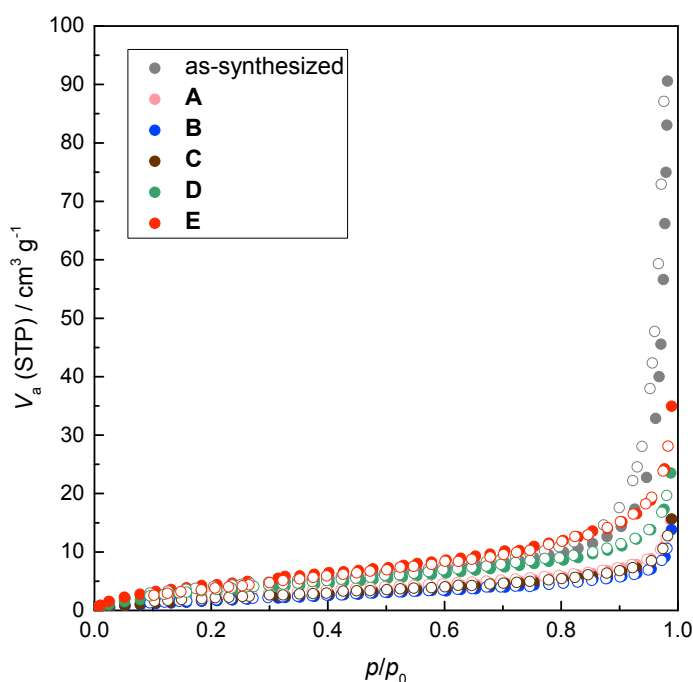

Figure S7　　N_2 adsorption isotherms of the as-synthesized [Sm(dehp)$_3$] and the cryogels **A–E**.

Barrett–Joyner–Halenda method, the increase in V_a should be caused by the presence of the pores of the size larger than ca. 10 nm. The average pore size was estimated to be 48 nm. Contrary to this, all the isotherms of the gels A–E are non-porous type. Despite of such a difference, the Brunauer–Emmett–Teller (BET) surface area (listed in Table S4) are not so different from each other because the specific surface area is originally small.

Table S4   BET surface area of the as-synthesized $[Sm(dehp)_3]$ and the cryogels **A–E**.

	BET surface area / $m^2\ g^{-1}$
as-synthesized	16
A	8.6
B	7.5
C	8.3
D	14
E	18

6. Ion exchange

The as-synthesized $[Sm(dehp)_3]$ and the cryogel **D** (R=54) (50 mg) were mixed with a $Ln(NO_3)_3$ aqueous solution (0.125 mM Ln=Ce, Nd, Eu, Dy, or Yb, 10 mL) with stirring at 20 °C. The supernatant solution was collected by filtration after specific time intervals, and the Ln^{3+} concentrations ($c(Ln^{3+})$) were measured using ICP-OES.

Figure S8 shows the time course of ln $c(Ln^{3+})/c^i(Ln^{3+})$, where $c^i(Ln^{3+})$ represents the initial concentration (i.e., 0.125 mM). The reactions seem to reach equilibrium at 350 and 680 h for the as-synthesized $[Sm(dehp)_3]$ and the cryogel **D**, respectively. Therefore, the distribution coefficient (K_d / L g^{-1}) was determined from the data at 680 h by the following equation:

$K_d = Q(Ln^{3+})/c(Ln^{3+})$

where $c(Ln^{3+})$ and $Q(Ln^{3+})$ are the concentrations of Ln^{3+} in the solution and solid phases, respectively. The $Q(Ln^{3+})$ was calculated based on the mass balance of Ln^{3+}. The results are shown in Figure 7(i) in the main article.

The pseudo-first-kinetic constant (k_1) was estimated from linear fitting of the data in the time range of 0-180 h, based on the following equation:

ln $c/c_0 = -k_1 \cdot t$

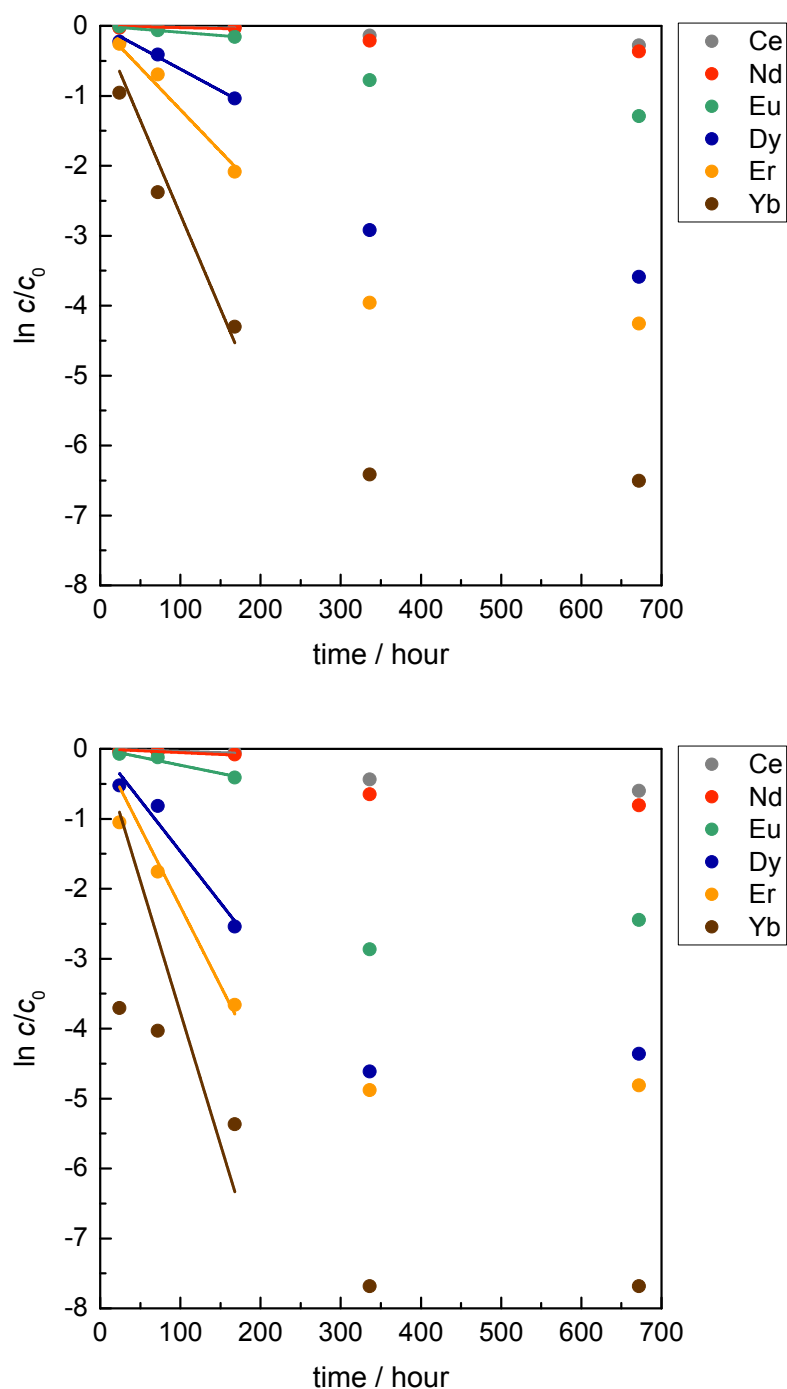where t represents time. The results are shown in Figure 7(ii) in the main article.

Figure S8   The change in ln $c(Ln^{3+})/c^i(Ln^{3+})$ with time for the as-synthesized [Sm(dehp)$_3$] (above) and the cryogel **D** (bottom).

Reference

1) R. J. Ellis, T. Demars, G. Liu, J. Niklas, O. G. Poluektov and I. A. Shkrob, *J. Phys. Chem. B*, 2015, 119, 11910–11927.

2) H. Shiwaku, T. Mitsui, K. Tozawa, K. Kiriyama, T. Harami, T. Mochizuki, *American Institute of Physics Conference Proceedings*, 2004, 705, 659.